Doubly stochastic coherence in complex neuronal networks

Yang Gao* and Jianjun Wang
College of Nuclear Science and Technology, Harbin Engineering University, Harbin, China, 150001
(Received 24 July 2012; revised manuscript received 15 October 2012; published 26 November 2012)

A system composed of coupled FitzHugh-Nagumo neurons with various topological structures is investigated under the co-presence of two independently additive and multiplicative Gaussian white noises, in which particular attention is paid to the neuronal networks spiking regularity. As the additive noise intensity and the multiplicative noise intensity are simultaneously adjusted to optimal values, the temporal periodicity of the output of the system reaches the maximum, indicating the occurrence of doubly stochastic coherence. The network topology randomness exerts different influences on the temporal coherence of the spiking oscillation for dissimilar coupling strength regimes. At a small coupling strength, the spiking regularity shows nearly no difference in the regular, small-world, and completely random networks. At an intermediate coupling strength, the temporal periodicity in a small-world neuronal network can be improved slightly by adding a small fraction of long-range connections. At a large coupling strength, the dynamical behavior of the neurons completely loses the resonance property with regard to the additive noise intensity or the multiplicative noise intensity, and the spiking regularity decreases considerably with the increase of the network topology randomness. The network topology randomness plays more of a depressed role than a favorable role in improving the temporal coherence of the spiking oscillation in the neuronal network research study.

DOI: 10.1103/PhysRevE.86.051914 PACS number(s): 87.10.−e, 89.75.−k

I. INTRODUCTION

Neurons are the fundamental units of our brain and various neuronal systems and they engage in complex and efficient signal-processing operations. A neuronal population can be modeled as a network or graph, where the nodes and edges represent specific neurons and interactions between them, respectively. Previous research analysis has shown that anatomical and functional brain networks [1–4] as well as corticocortical connections in the macaque and cat [5,6] exhibit a small-world topology [7]. So far, a wide variety of dynamical behaviors in small-world neural networks [8–13] have been investigated intensively. For instance, it has been demonstrated that networks of Hodgkin-Huxley neurons with small-world topologies give rise to a fast system response with coherent oscillations [9]. Economic small worlds are efficient in propagating information both on a local and global scale [10]. A noisy small-world neuronal network with delay and diversity can induce fruitful synchronization transitions [12]. A dominant phase-advanced driving method has been proposed to reveal the self-sustained oscillations of target waves in excitable small-world networks [13]. All these studies imply that the dynamics of a neuronal network is closely connected with its structure.

Noise is present inevitably in real signal transmission and transduction and constitutes a significant component of neural activity. It has been documented that sometimes noise can have constructive effects on the dynamical behaviors of neuronal systems. A couple of examples include noise-induced pattern formation [14,15], noise-induced phase transition to excitability [16], as well as noise-sustained and controlled synchronization [17]. In particular, the phenomena of stochastic resonance (SR) [18] and coherence resonance (CR) [19] have been studied extensively in individual neurons, single neural networks, and coupled neural networks. The evidence has shown that noise can help the sensory mechanoreceptors of crayfish detect a very weak water movement of about 10 nm [20]. Human sensory perception can be improved considerably by means of SR [21]. Experimental evidence of CR has been reported in the cat's anesthetized system [22]. The spatial coherence resonance has been studied in neuronal media which is locally modeled by a two-dimensional iterated map [23]. The occurrence of multiple stochastic resonances [24,25] and multiple coherence resonances have been demonstrated also in neuronal networks [26].

Sensory neurons transform signals from the environment into trains of spike that propagate to other structures in the neural system. Whether neurons can quickly and efficiently transmit signals depends on the spiking regularity to a great extent. Therefore, various excitable neuron models have been proposed to investigate the spiking activity of a neuron, among them FitzHugh-Nagumo (FHN) model [27] serving as a paradigm due to its simplicity and capturing the salient features of the neuron dynamics. The effect of CR has been demonstrated in the single FHN neuron [19] and in a heterogeneous array of coupled FHN neurons [28]. Spiking behavior combining oscillatory and excitable properties has also been studied in a noise-driven FHN neuron system [29]. Furthermore, doubly stochastic coherence (DSC), a type of stochastic resonancelike behavior, has been observed in an asymmetrically bistable FHN model under the joint action of multiplicative and additive noises [30]. Actually, many systems, especially neurobiological systems, are subject to additive noise and multiplicative noise simultaneously, and thus the DSC phenomenon could be of importance for understanding the mechanism of coherence motion in neural and biological systems.

In this paper, we also examine the DSC phenomenon in systems of coupled FHN neurons with different topologies. It is discovered that DSC can occur in the regular, small-world, and completely random neuronal networks at weak and

*Corresponding author: gaoyang@hrbeu.edu.cn

moderate coupling between individual neurons. Moreover, the temporal coherence of the excitable system can be enhanced only to a very limited extent by optimizing the additive noise intensity, the multiplicative noise intensity, and the topological randomness simultaneously. At a large coupling, the spiking regularity completely loses the resonance characteristic with regard to the additive noise intensity or the multiplicative noise intensity, as well as decreases with an increase of the disorder of the network topological structure.

II. MODEL AND METHODS

The model employed here consists of an array of FHN neurons in which a small-world network topology is constructed as follows. First, a regular lattice is considered which comprises N ($N = 100$) identical FHN neurons. Each neuron connects to its k ($k = 4$) nearest neighbors. Next, each local link is visited once and, with the rewiring probability p, removed and reconnected to a randomly chosen neuron. The limit cases of regularity and complete randomness are for $p = 0$ and $p = 1$, respectively, and the small-world topology lies somewhere in the intermediate region $0 < p < 1$. It should be noted that many network realizations exist for a given p.

The dynamics of a single FHN neuron can be described by the following equations:

$$\varepsilon \frac{dx}{dt} = x(1-x)(x-a) - y, \tag{1}$$

$$\frac{dy}{dt} = bx - y - xy\xi(t) + \zeta(t), \tag{2}$$

where $x(t)$ is a fast voltage variable representing the membrane voltage of the neuron, and $y(t)$ is a slow recovery variable relating to the time-dependent conductance of the potassium channels in the membrane. The time constant ε determines the speed of the firing process. $\xi(t)$ and $\zeta(t)$ are the mutually uncorrelated multiplicative and additive Gaussian noises with zero mean and correlations $\langle \xi(t)\xi(t')\rangle = 2D_m\delta(t-t')$ and $\langle \zeta(t)\zeta(t')\rangle = 2D_a\delta(t-t')$. D_m and D_a are the strength of $\xi(t)$ and $\zeta(t)$, respectively. The parameters are $a = 0.15$, $b = 0.12$, and $\varepsilon = 0.01$. Here all the quantities are dimensionless.

For a single deterministic FHN neuron, there are two stable fixed points with different stabilities (see curve 1 and its crossing points with the x nullcline in Fig. 1). As the role of multiplicative noise is to adjust the symmetric response of the system and additive noise is responsible for causing jumps between the two stable steady states [30], the stabilities of the two states are almost the same for an intermediate multiplicative noise intensity (see curve 2 in Fig. 1), but are quite different for a large multiplicative noise strength (see curves 3 in Fig. 1). Figures 2(a)–2(c) show the time series of x for the corresponding parameters in curves 1, 2, and 3 of Fig. 1, respectively. The time series are obtained from numerical integration of the stochastic differential equations (1) and (2) using the Euler scheme with a fixed time step of 0.002. It can be seen that for both zero and a large value

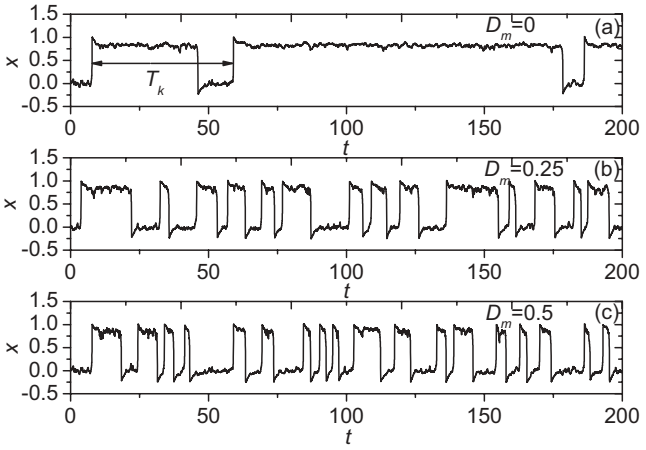

FIG. 2. (a)–(c) The time series of x for the corresponding parameters in curves 1, 2, and 3 of Fig. 1.

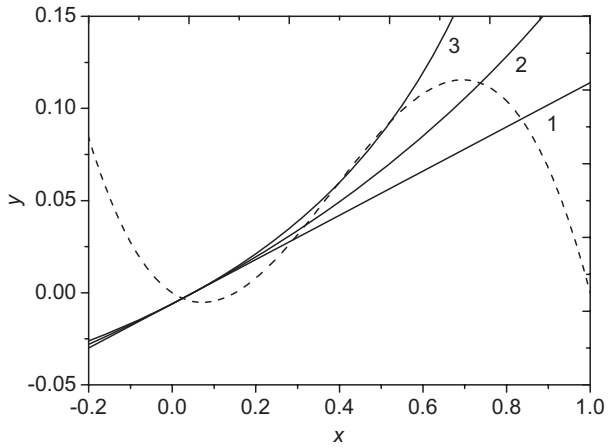

FIG. 1. Nullcline plot of the FHN model. Dashed line: x nullcline ($\dot{x} = 0$). Solid lines: y nullclines ($\dot{y} = 0$) for three different multiplicative noise intensities: $D_m = 0$ (curve 1), $D_m = 0.25$ (curve 2), and $D_m = 0.5$ (curve 3). The additive noise intensity is $D_a = 0.014$; other parameters are given in the text.

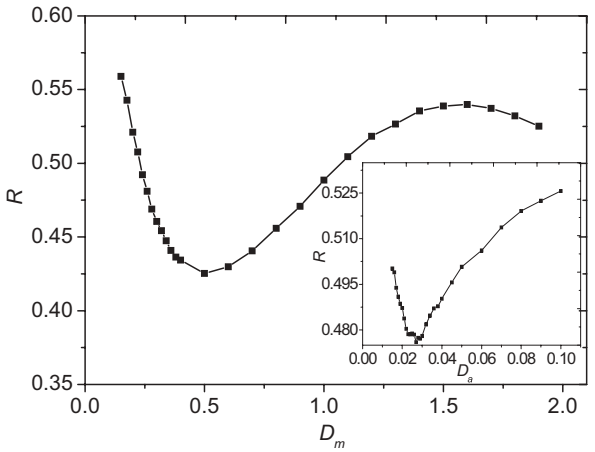

FIG. 3. The coherence factor R vs the multiplicative noise intensity D_m and the additive noise intensity D_a (inset plot). $D_a = 0.02$ and $D_m = 0.25$, respectively. The rewiring probability $p = 0.1$, and the coupling strength $g = 0.01$.

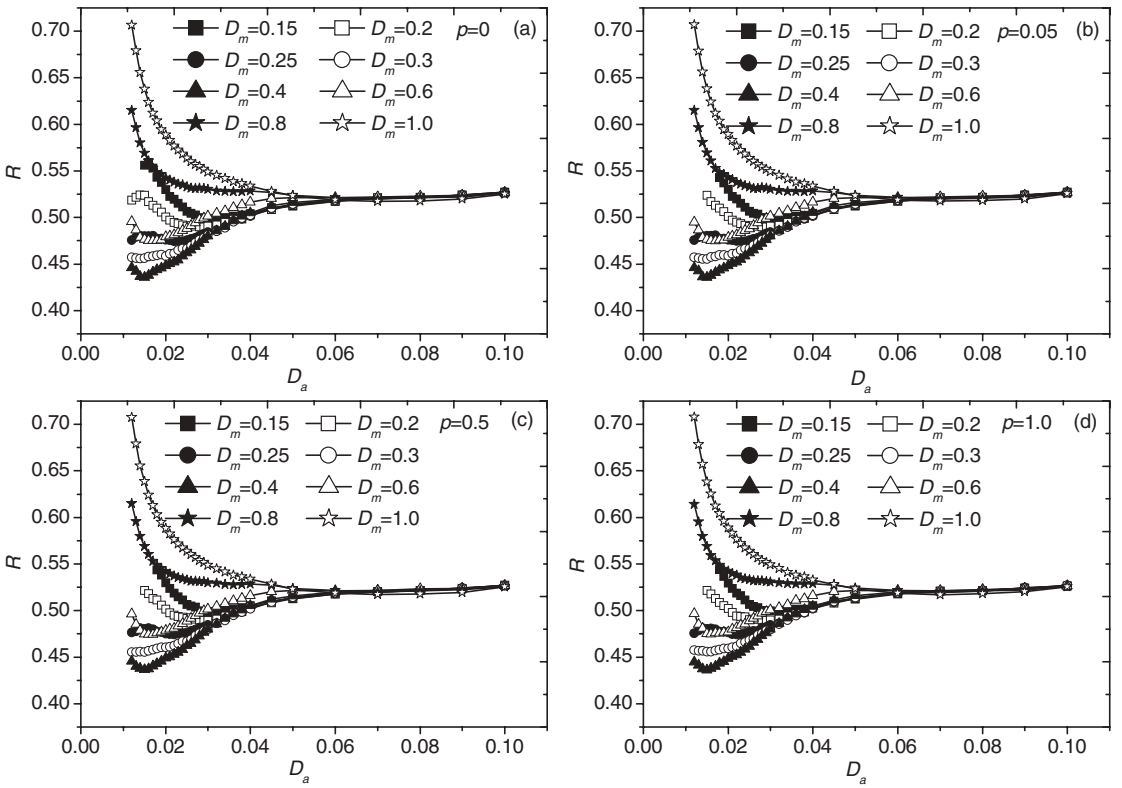

FIG. 4. The coherence factor R against the additive noise intensity D_a at different multiplicative noise strengths D_m with (a) $p = 0$, (b) $p = 0.05$, (c) $p = 0.5$, and (d) $p = 1.0$. The coupling strength is $g = 0.001$.

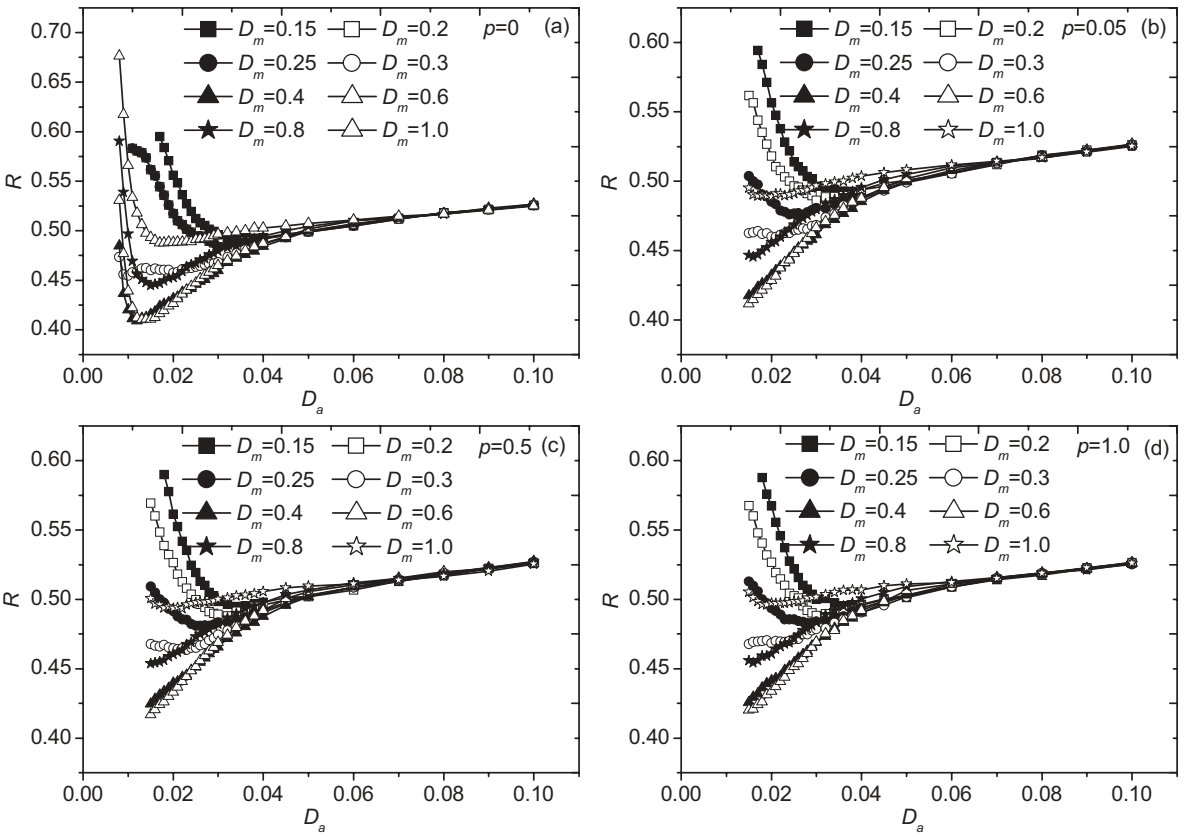

FIG. 5. The coherence factor R against the additive noise intensity D_a at different multiplicative noise strengths D_m with (a) $p = 0$, (b) $p = 0.05$, (c) $p = 0.5$, and (d) $p = 1.0$. The coupling strength is $g = 0.01$.

of D_m, the system spends more time in the upper and lower states, respectively, while for the moderate multiplicative noise intensity, the system spends almost equal time in the two states, and the oscillation in the time series seems to be more regular compared to the two cases above.

The differential equations describing the neurons in a coupled network are given by

$$\varepsilon \frac{dx_i}{dt} = x_i(1-x_i)(x_i-a) - y_i + \frac{g_{ij}}{2}(x_j - x_i), \quad (3)$$

$$\frac{dy_i}{dt} = bx_i - y_i - xy\xi_i(t) + \zeta_i(t). \quad (4)$$

Here i and j running from 1 to N are the numbers of the neurons. g_{ij} is the coupling parameter between the two neurons i and j, and its value is determined by the coupling pattern of the system. If these two neurons are coupled to each other, g_{ij} is a determinate value g; otherwise, $g_{ij} = 0$.

To characterize the temporal coherence of the oscillation in a neuron quantitatively, the coherence factor R_i [19] of the variable x_i is obtained by the following formula:

$$R_i = \frac{\sqrt{\mathrm{var}\,(T_k)}}{\langle T_k \rangle}. \quad (5)$$

The meaning of T_k is illustrated in Fig. 2(a). R can be interpreted, in the context of stochastic resonance terminology, as the signal-to-noise ratio (SNR) [19]. A smaller R_i corresponds to a better coherence. Here we focus on the collective behavior of the network and measure the average factor R,

$$R = [\langle R_i \rangle], \quad (6)$$

where $\langle\cdot\rangle$stands for the average of all the neurons and $[\cdot]$ denotes averaging over 30 different network realizations for each p.

III. RESULTS AND DISCUSSIONS

Figure 3 and its inset show that increasing the multiplicative noise intensity D_m or the additive noise intensity D_a first increases then suppresses the temporal coherence of the output (the value of R initially decreases then increases). In other words, when the intensity of either of the two noises is fixed, the other one induces a favorable temporal coherence of the oscillation with a suitable strength. No doubt there could exist an optimal set of multiplicative noise intensity and additive noise intensity which corresponds to the best regularity in the system oscillation, which is the origin of doubly stochastic coherence.

Figures 4(a)–4(d) plot the coherence factor R against the additive noise intensity D_a achieved at different multiplicative noise strengths D_m and rewiring probabilities p when the coupling strength between the units is weak ($g = 0.001$). It can be observed that R in all the curves first decreases and then increases with an increase of D_a, implying the occurrence of CR. The maximal coherence factor of each curve is signed by R_{opt1}, and the noise intensity at R_{opt1} is called the

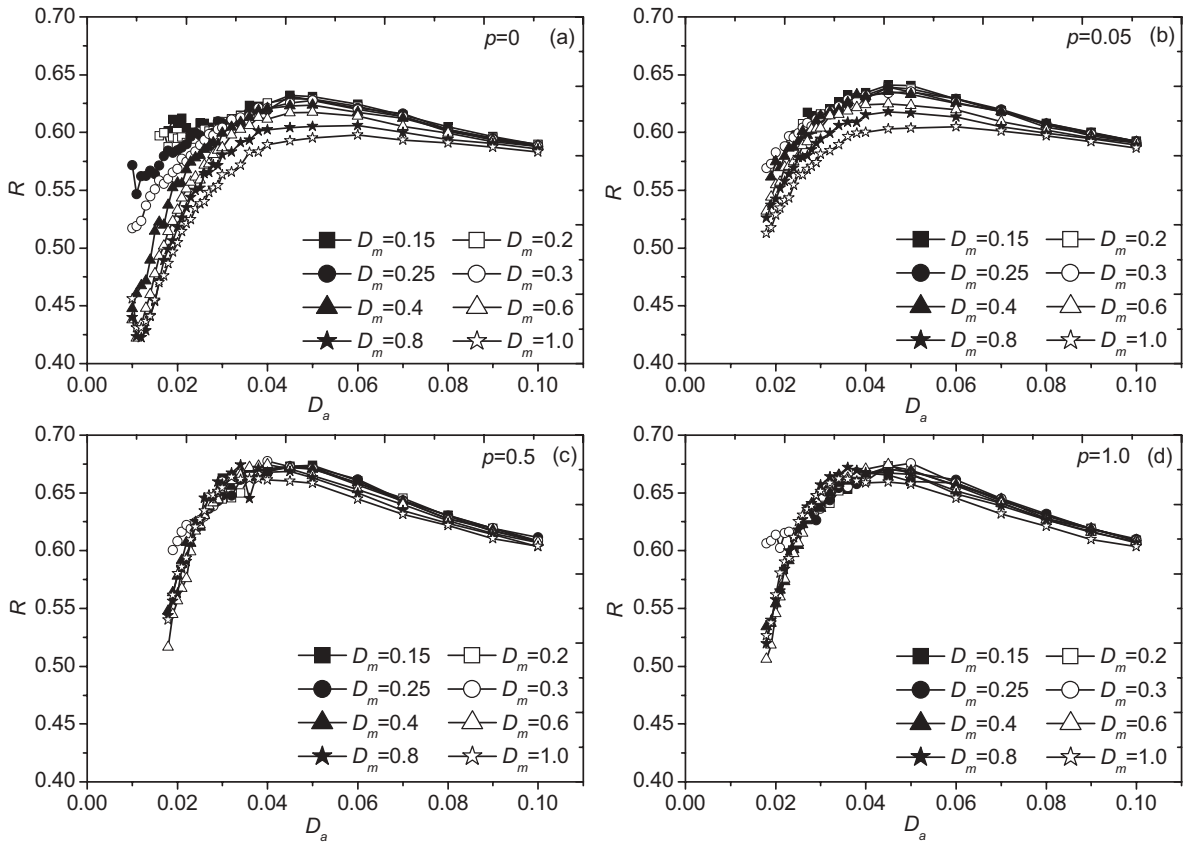

FIG. 6. The coherence factor R against the additive noise intensity D_a at different multiplicative noise strengths D_m with (a) $p = 0$, (b) $p = 0.05$, (c) $p = 0.5$, and (d) $p = 1.0$. The coupling strength is $g = 0.05$.

optimal additive noise intensity D_{opt1}. Both R_{opt1} and D_{opt1} are the smallest at $D_m = 0.4$ in each plot of Fig. 4, indicating that, regardless of the rewiring probability p, there exists an identical optimal multiplicative noise level at which the most ordered oscillation can be induced by the weakest additive noise. Similar results are obtained for $g = 0.005$ and the corresponding figures are omitted. The plots in Fig. 5 illustrate two different cases of R vs D_a when the coupling strength increases to 0.01. For a regular neuronal network ($p = 0$), the phenomenon of CR will occur regardless of the value of D_m. However, when the rewiring probability p is nonzero, only for the smaller multiplicative noise strengths ($D_m = 0.15, 0.2,$ and 0.25), the R-D_a curves present a typical CR characteristic; otherwise, R nearly rises monotonously with increasing D_a at a fixed D_m. The dynamical behavior of the neurons at $g = 0.05$ completely loses the CR property, instead showing the "anticoherence resonance" feature whether the neurons are in one of the networks with regular, small-world, or completely random topologies. As depicted in the plots of Fig. 6, each curve of R against D_a has a maximum which represents the worst temporal coherence.

Figures 7–9 show how the coherence factor R changes with the multiplicative noise intensity D_m at different additive noise strengths D_a and rewiring probabilities p for the corresponding coupling strengths in Figs. 4–6, respectively. When $g = 0.001$, except at $D_a = 0.04$ and 0.05 where the value of R has a low dependence on D_m, there is a smallest R value in each R-D_m curve at other additive noise intensities. Here the minimum of R is marked as R_{opt2}, and the noise intensity at R_{opt2} is termed the optimal multiplicative noise intensity D_{opt2}. It can be clearly observed from the plots of Fig. 7 that the optimal level of the additive noise is $D_a = 0.015$. When g increases to 0.01, the collective behaviors of the neuronal networks are basically the same as $g = 0.001$, with just the value of the optimal additive noise intensity being slightly smaller ($D_a = 0.0125$). In the case of $g = 0.05$, the coherence factor R as a function of D_m differs from those at the other coupling intensities. Only a few curves in Fig. 9 can display an observable CR characteristic, such as that for $p = 1.0$ and $D_a = 0.175$, and the phenomenon of coherence resonance nearly disappears in most cases.

As discussed above, the temporal periodicity of the collective oscillation can present a typical CR characteristic with regard to the additive or multiplicative noise intensity in the cases with smaller coupling strength. Therefore, the phenomenon of doubly stochastic coherence can appear only at weak or moderate coupling between individual neurons. The counter plots of R for various D_a and D_m in Fig. 10 distinctly show the DSC behavior in the regular, small-world, and completely random neuronal networks, respectively. Here the coupling strength $g = 0.01$ is taken as an example. The DSC region seems to decrease alongside the increase of the disorder degree of the network.

The research focused extensively on the effects of the network topological structure on the dynamical property of the system. Figures 11 and 12 display separately the dependence of R on D_a and D_m achieved at various network randomnesses. The selected fixed multiplicative or additive

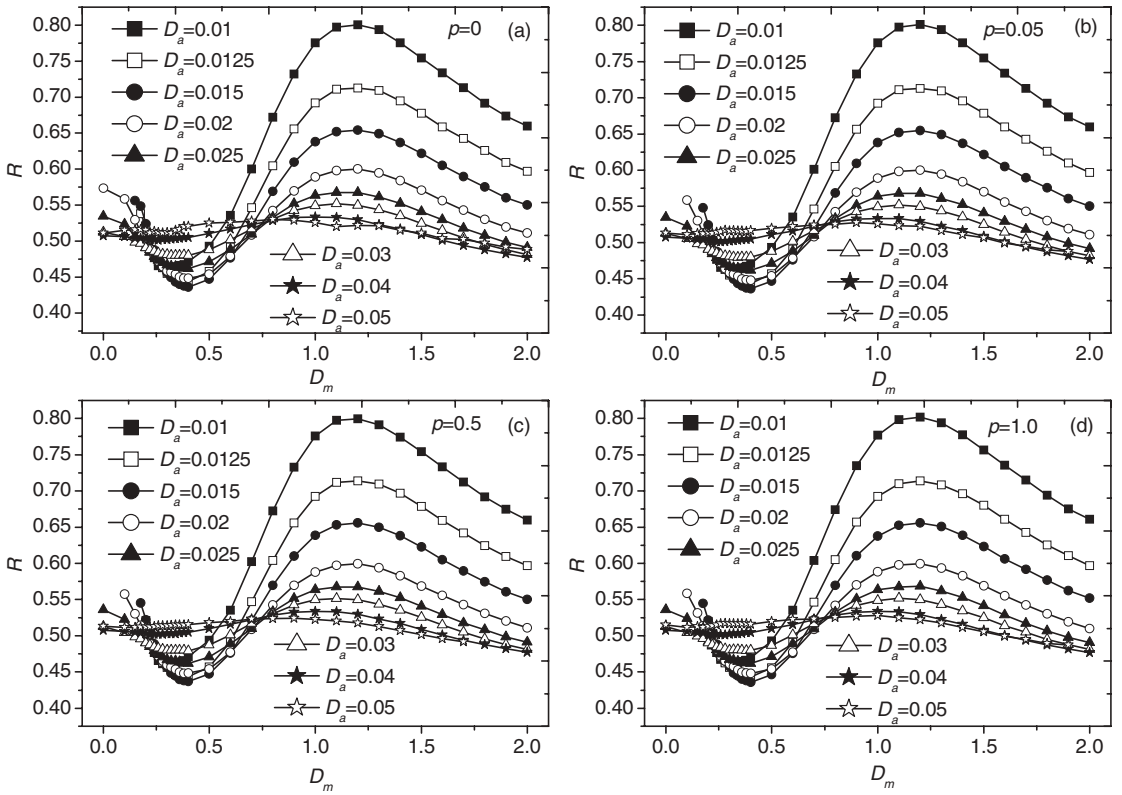

FIG. 7. The coherence factor R against the multiplicative noise intensity D_m at different additive noise strengths D_a with (a) $p = 0$, (b) $p = 0.05$, (c) $p = 0.5$, and (d) $p = 1.0$. The coupling strength is $g = 0.001$.

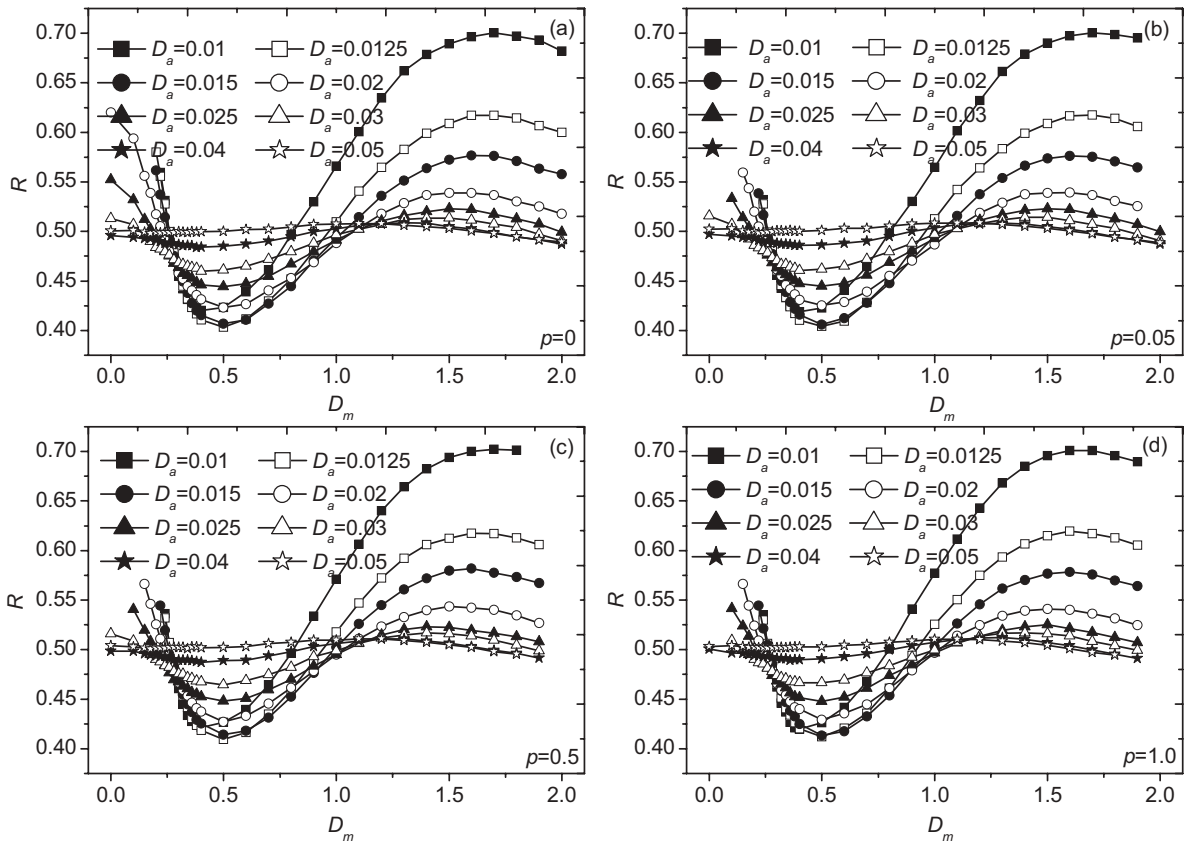

FIG. 8. The coherence factor R against the multiplicative noise intensity D_m at different additive noise strengths D_a with (a) $p = 0$, (b) $p = 0.05$, (c) $p = 0.5$, and (d) $p = 1.0$. The coupling strength is $g = 0.01$.

noise intensities are $D_m = 0.2$, 0.4, 0.8 and $D_a = 0.015$, 0.025, 0.05, respectively. The solid, dashed, and dotted lines in each plot denote the cases of different coupling strengths. When $g = 0.001$, the curves at different rewiring probabilities in Fig. 11 almost overlap regardless of the value of D_m, indicating that the influence of the network topology on the system's dynamical behavior is meager at such a weak coupling. In these cases, each neuron is almost independent and behaves as if it is isolated, so the topological structure has little influence on the temporal coherence of the system's oscillation. When g increases to 0.01, although the change of R_{opt1} with the increase of p is not very obvious at $D_m = 0.2$, one can still discern that the smallest value of R_{opt1} appears at $p = 0.1$ from Fig. 11(a) [see the inset in Fig. 11(a) for a clearer view], implying that the increment of the disorder of the network topological structure plays some positive role in enhancing CR and there is an optimal rewiring probability around $p = 0.1$. As for the cases of $D_m = 0.4$ and $D_m = 0.8$, the dependence of R on p is a bit strong when D_a is small, while this dependency weakens at large D_a. Furthermore, no coherence resonance phenomenon happens in these two cases except in the regular network at $D_m = 0.4$. When the coupling strength increases further to $g = 0.05$, the phenomenon of "anticoherence resonance" instead of coherence resonance appears in the networks. Moreover, increasing the randomness of the network suppresses the spiking regularity of the neurons, and the coherent factor R rises as the rewiring probability p increases on the whole when all the other parameters are fixed. In our previous studies on CR of coupled neuronal systems it has been found that at a strong coupling the coherence motion is depressed with the increment of long-range connections [31,32], and a similar result is obtained here.

The effect law of the network topology on the dynamical behavior of the neuronal system in Fig. 12 is similar to the findings shown in Fig. 11. Increasing the network topology randomness has a little, limitedly positive, or considerably adverse impact on the enhancement of the spiking regularity of the neuronal network at weak, intermediate, or strong couplings, respectively. Furthermore, when comparing the curves of R-D_a or R-D_m in different line styles in each plot of Figs. 11 and 12, it can be obvious to find that $g = 0.01$ is a favorable coupling strength. R vs D_a and R vs D_m at different g are plotted in Figs. 13(a) and 13(b), respectively, where $p = 0.05$ is taken as an example. It can be seen that both R_{opt1} and R_{opt2} have the smallest values at $g = 0.01$, which further assures that $g = 0.01$ is the optimal coupling strength.

In prior work it has been established that long-range connections are favorable for the emergence of temporal coherence. For example, the random connectivity of the networks may induce improvement in both temporal stochastic resonance and spatial synchronization of the bistable oscillators [33]. In the coupled Hodgkin-Huxley neurons, there are optimal random shortcuts where the collective spike coherence and the individual one conduct the best temporal coherence [34]. Only

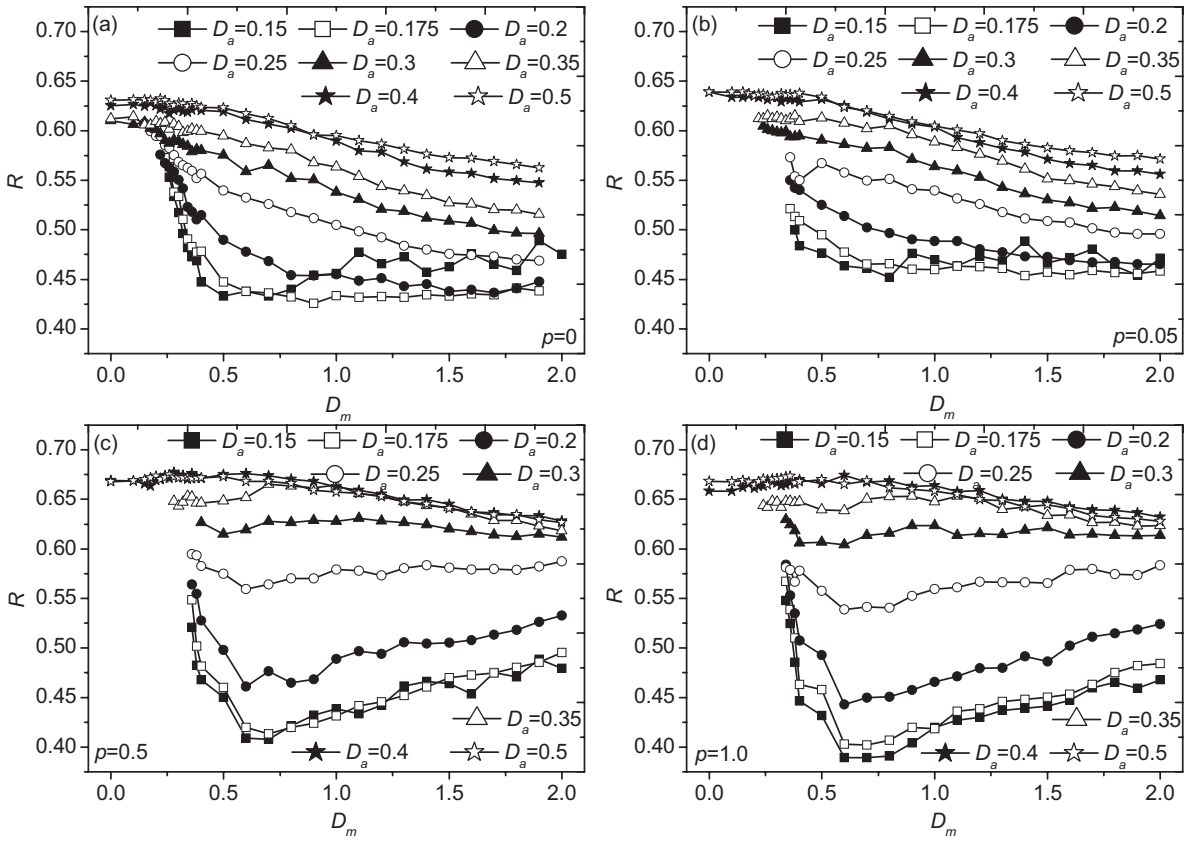

FIG. 9. The coherence factor R against the multiplicative noise intensity D_m at different additive noise strengths D_a with (a) $p = 0$, (b) $p = 0.05$, (c) $p = 0.5$, and (d) $p = 1.0$. The coupling strength is $g = 0.05$.

for intermediate coupling strengths is the small-world property able to improve the stochastic resonance [35] and the coherence resonance [36] in the excitable small-world networks. The stochastic resonance on a Newman-watts network of Hodgkin-Huxley neurons with local periodic driving can be further amplified via fine tuning of the small-world network structure [37]. Here it is also found that doubly stochastic coherence of the neuronal network can be enhanced by introducing long-range connections into the system. Usually a small-world network is characterized by two main properties: That is, it has a large clustering coefficient as a regular network, while at the same time having a short characteristic path length similar to a completely random network. The clustering coefficient is defined as the extent to which nodes connected to any node in a network are connected to each other. The characteristic path length represents the number of edges in the shortest path between two nodes of a network, averaged over all node pairs. So in a small-world neuronal network, each neuron may have more "close neighbors," and its signals will propagate more quickly to a larger number, leading to an increase of the spiking coherence.

However, it should be noted that compared with the previous results, the advantage of small-world topology on the improvement of the temporal coherence has been reduced greatly in this study. Especially in the case of strong coupling, the spiking regularity in the neurons is destroyed as the randomness of the network topology increases, and the resonance property in the system no longer exists. Interestingly, it has been demonstrated that small-world network topology suppresses spatial coherence [38–40]. Here, combining the viewpoints of Zaikin *et al.* [30] and Perc [40], the phenomenon above might be understood in this way: The additive noise can be more effective in producing temporal coherence if only an optimal level of multiplicative noise induces a symmetric bistable state in a neuron. In a regular network, each neuron connects to its nearest four neighbors by undirected edges, and the coupling strength between two coupled neurons is identical. The symmetric response in a neuron is mainly influenced by the multiplicative noise injected into it and the coupling strength. Therefore, the DSC phenomenon can usually occur in a regular coupled network provided that the multiplicative noise level is suitable and the coupling strength is not too large. At a strong coupling, all neurons tend to behave as a single one, and it is difficult to induce resonance phenomenon for "a single neuron" subjected to no less than 100 additive or multiplicative noise sources, just as it is shown in Figs. 6(a) and 9(a). In a small-world network, although the total number of connections remains constant regardless of the rewiring probability, the number of connections of each neuron could be very different from one another as if the coupling between neurons varies from unit to unit; this to some extent disrupts the spatial bistable state of the excitable system. Thus, in general, the regularity of the spiking oscillation in a small-world network does not show any advantage over that in a regular network, or even if there is some advantage, it is rather limited.

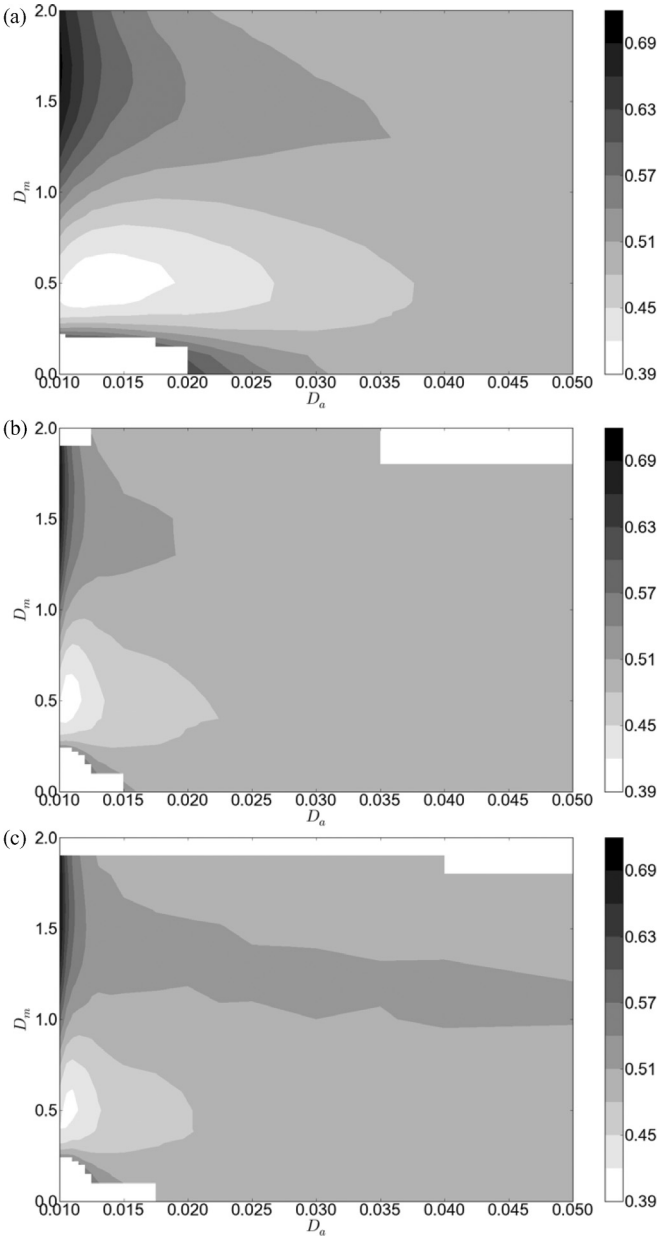

FIG. 10. The counter plots of the coherence factor R vs the additive noise intensity D_a and the multiplicative noise intensity D_m (lighter gray corresponds to a smaller value of R) with (a) $p = 0$, (b) $p = 0.1$, and (c) $p = 1.0$. The coupling strength is $g = 0.01$.

IV. SUMMARY

In this paper, numerical simulations are presented for the collective dynamical behavior of an array of coupled FitzHugh-Nagumo neurons with various topological structures. Each neuron is subjected to two independently additive and multiplicative sources of noise. The results show that the spiking regularity of the network can be maximized by simultaneously optimizing the additive noise intensity D_a and the multiplicative noise intensity D_m, indicating the occurrence of doubly stochastic coherence. The temporal coherence of the spiking oscillation in the system has a strong dependence on the coupling between neurons. The phenomenon of doubly stochastic coherence can fully surface only when the coupling

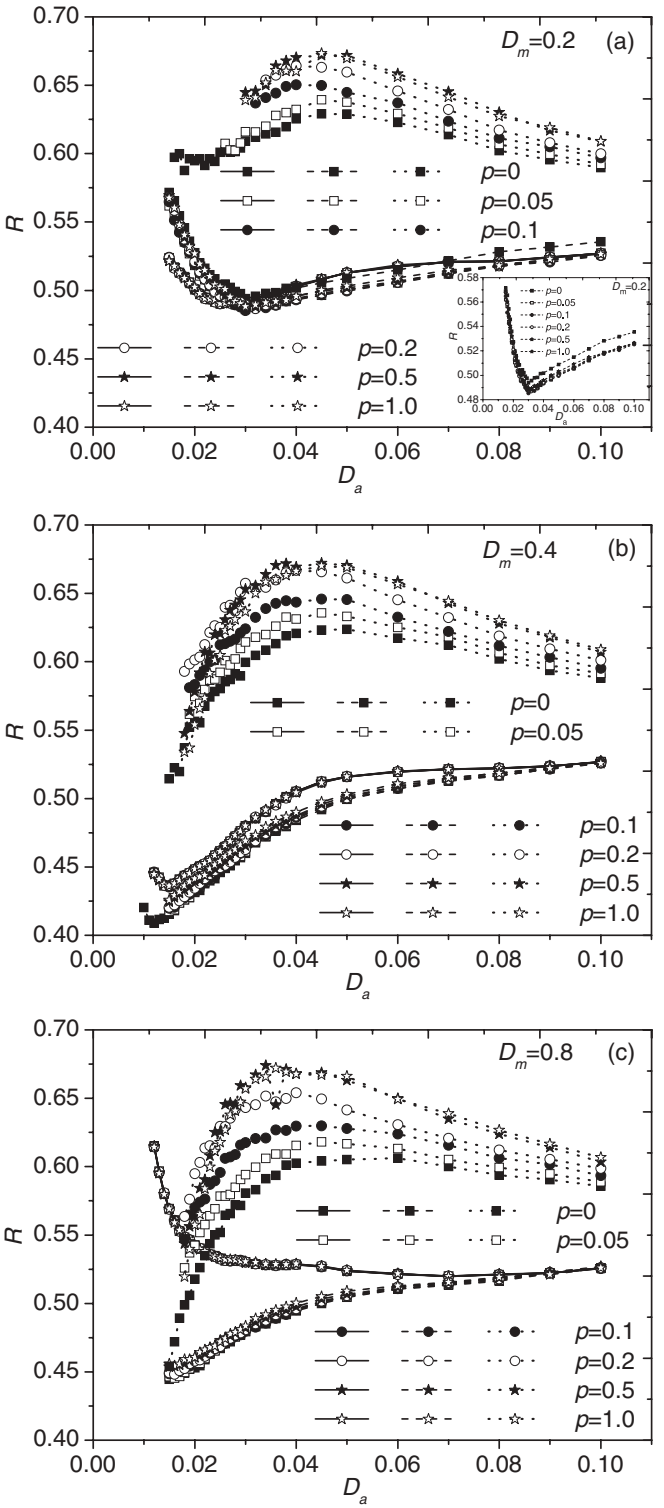

FIG. 11. The coherence factor R vs the additive noise intensity D_a at different rewiring probabilities p with (a) $D_m = 0.2$, (b) $D_m = 0.4$, and (c) $D_m = 0.8$. The solid, dashed, and dotted lines denote the cases of coupling strength $g = 0.001$, 0.01, and 0.05, respectively.

remains at a smaller strength level. As the coupling strength is large, there is the threat of totally losing the coherence resonance property with regard to D_a or D_m. The network topological structure exerts dissimilar influences on the spiking

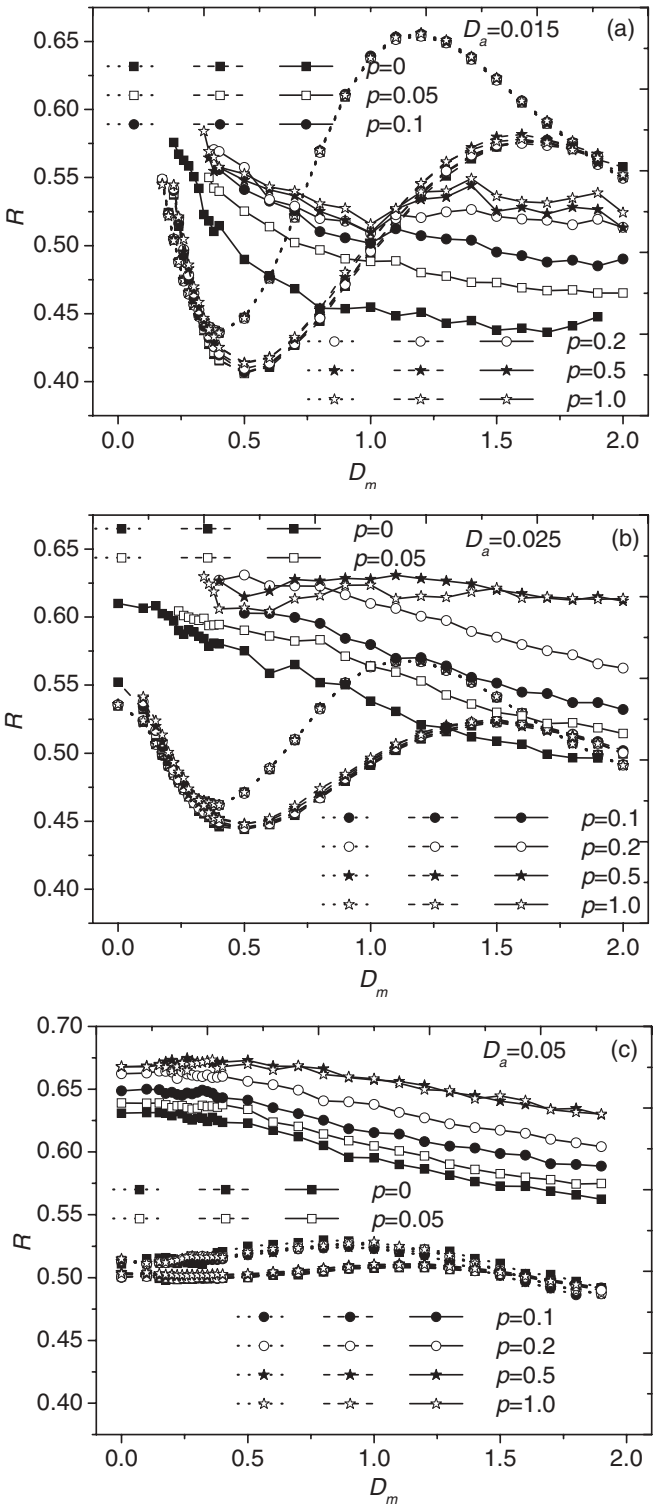

FIG. 12. The coherence factor R vs the multiplicative noise intensity D_m at different rewiring probabilities p with (a) $D_a = 0.015$, (b) $D_a = 0.025$, and (c) $D_a = 0.05$. The dotted, dashed, and solid lines denote the cases of coupling strength $g = 0.001, 0.01$, and 0.05, respectively.

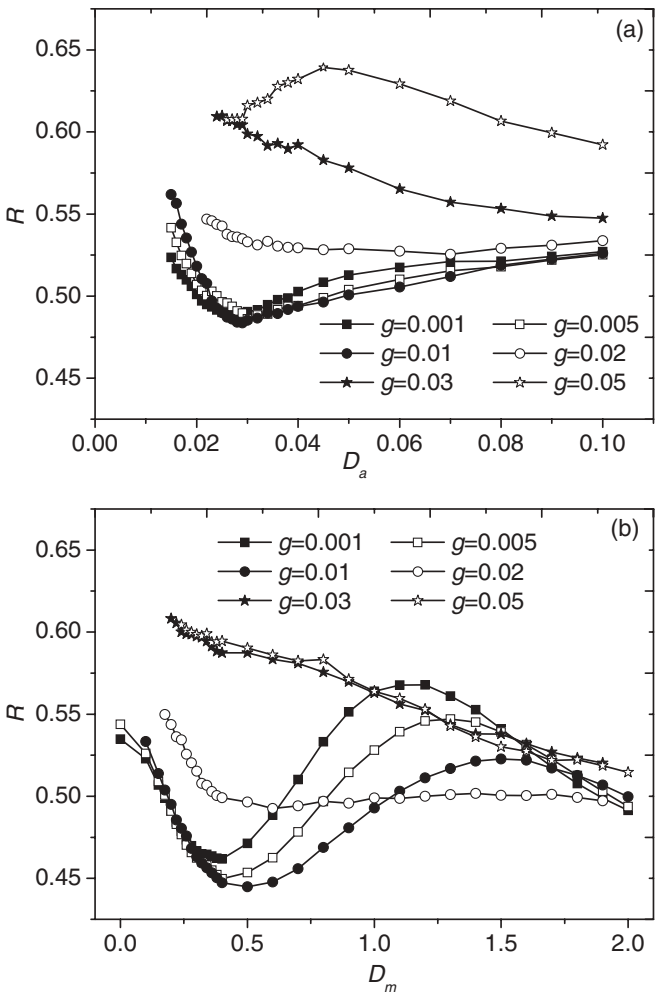

FIG. 13. (a) The coherence factor R vs the additive noise intensity D_a and (b) the coherence factor R vs the multiplicative noise intensity D_m at different coupling strengths g. The rewiring probability is $p = 0.5$.

regularity for various coupling strength regimes. At a low coupling strength, the temporal coherence shows almost no difference in the regular, small-world, and completely random networks. At an intermediate coupling strength, the temporal coherence in a small-world neuronal network can be improved by adding a small fraction of long-range connections; however, the enhancement degree is very limited even if all the control parameters are adjusted to optimum performance. At a large coupling strength, the regularity of the collective oscillation is considerably decreased with an increase of the network topology randomness. In general, the small-world network topology plays more of a negative rather than a positive role in improving the temporal coherence of the spiking oscillation in our neuronal network. The basic reason for this situation could be that the long-range connections have a favorable effect on the temporal noise-induced coherence but a destructive impact on the spatial symmetry of the bistable state. Good symmetry of the two stable steady states is just the precondition for producing favorable temporal coherence.

Furthermore, the dynamics of the coupled neuronal ensembles are synchronous in the research. In fact, there exist time delays as neurons communicate and transmit information to each other. Recent studies have shown that temporal delays have negative effects on the coherence of noise-induced spatial dynamics on small-world neuronal networks [41,42]. The

question to ask is how this will affect the dynamics of the used model in terms of time delays by the small-world topology and what the degree of the effect is. Further research will be made along such a direction and some different phenomena are expected to be uncovered.

ACKNOWLEDGMENTS

This work was supported by the School Fund of Harbin Engineering University (002150260705) and by the Special Fund of Central University Basic Scientific Research Fee (GK2150260105).

[1] O. Sporns, D. R. Chialvo, M. Kaiser, and C. C. Hilgetag, Trends Cogn. Sci. **8**, 418 (2004).
[2] D. S. Bassett and E. Bullmore, Neuroscientist **12**, 512 (2006).
[3] J. C. Reijneveld, S. C. Ponten, H. W. Berendse, and C. J. Stam, Clin. Neurophysiol. **118**, 2317 (2007).
[4] C. J. Stam and J. C. Reijneveld, Nonlin. Biomed. Phys. **1**, 3 (2007).
[5] J. W. Scannell, Nature (London) **386**, 452 (1997).
[6] J. W. Scannell, C. Blakemore, and M. P. Young, J. Neurosci. **15**, 1463 (1995).
[7] D. J. Watts, *Small Worlds: The Dynamics of Networks Between Order and Randomness* (Princeton University Press, Princeton, NJ, 1999).
[8] S. Boccaletti, V. Latora, Y. Moreno, M. Chavez, and D.-U. Hwang, Phys. Rep. **424**, 175 (2006).
[9] L. F. Lago-Fernández, R. Huerta, F. Corbacho, and J. A. Sigüenza, Phys. Rev. Lett. **84**, 2758 (2000).
[10] V. Latora and M. Marchiori, Eur. Phys. J. B **32**, 249 (2003).
[11] D. Wu, S. Zhu, X. Luo, and L. Wu, Phys. Rev. E **84**, 021102 (2011).
[12] J. Tang, J. Ma, M. Yi, H. Xia, and X. Yang, Phys. Rev. E **83**, 046207 (2011).
[13] Y. Qian, X. Huang, G. Hu, and X. Liao, Phys. Rev. E. **81**, 036101 (2010).
[14] H. Busch and F. Kaiser, Phys. Rev. E **67**, 041105 (2003).
[15] M. Perc, Eur. J. Phys. **27**, 451 (2006).
[16] E. Ullner, A. Zaikin, J. García-Ojalvo, and J. Kurths, Phys. Rev. Lett. **91**, 180601 (2003).
[17] C. Zhou and J. Kurths, New J. Phys. **7**, 18 (2005).
[18] R. Benzi, A. Sutera, and A. Vulpiani, J. Phys. A: Math. Gen. **14**, L453 (1981).
[19] A. S. Pikovsky and J. Kurths, Phys. Rev. Lett. **78**, 775 (1997).
[20] J. K. Douglass, L. Wilkens, E. Pantazelou, and F. Moss, Nature (London) **365**, 337 (1993).
[21] J. J. Collins, T. T. Imhoff, and P. Grigg, Nature (London) **383**, 770 (1996).
[22] E. Manjarrez, J. G. Rojas-Piloni, I. Méndez, L. Martínez, D. Vélez, D. Vázquez, and A. Flores, Neurosci. Lett. **326**, 93 (2002).
[23] M. Perc, Chaos, Solitons Fractals **31**, 64 (2007).
[24] Q. Wang, M. Perc, Z. Duan, and G. Chen, Chaos **19**, 023112 (2009).
[25] C. Gan, M. Perc, and Q. Wang, Chin. Phys. B **19**, 040508 (2010).
[26] Q. Wang, H. Zhang, M. Perc, and G. Chen, Commun. Nonlinear Sci. Numer. Simulat. **17**, 3979 (2012).
[27] R. A. FitzHugh, Biophys. J. **1**, 445 (1961).
[28] C. Zhou, J. Kurths, and B. Hu, Phys. Rev. Lett. **87**, 098101 (2001).
[29] V. A. Makarov, V. I. Nekorkin, and M. G. Velarde, Phys. Rev. Lett. **86**, 3431 (2001).
[30] A. Zaikin, J. García-Ojalvo, R. Báscones, E. Ullner, and J. Kurths, Phys. Rev. Lett. **90**, 030601 (2003).
[31] Q. Li and Y. Gao, Biophys. Chem. **130**, 41 (2007).
[32] Q. Li and Y. Gao, Phys. Rev. E **77**, 036117 (2008).
[33] Z. Gao, B. Hu, and G. Hu, Phys. Rev. E **65**, 016209 (2001).
[34] Y. Gong, M. Wang, Z. Hou, and H. Xin, Chem. Phys. Chem. **6**, 1042 (2005).
[35] M. Perc, Phys. Rev. E **76**, 066203 (2007).
[36] O. Kwon, H.-H. Jo, and H.-T. Moon, Phys. Rev. E **72**, 066121 (2005).
[37] M. Ozer, M. Perc, and M. Uzuntarla, Phys. Lett. A **373**, 964 (2009).
[38] X. Sun, M. Perc, Q. Lu, and J. Kurths, Chaos **18**, 023102 (2008).
[39] M. Perc, Chaos, Solitons Fractals **31**, 280 (2007).
[40] M. Perc, New J. Phys. **7**, 252 (2005).
[41] Q. Wang, M. Perc, Z. Duan, and G. Chen, Int. J. Mod. Phys. B **24**, 1201 (2010).
[42] Q. Wang, M. Perc, Z. Duan, and G. Chen, Phys. Lett. A **372**, 5681 (2008).